16th World Conference on Earthquake, 16WCEE 2017
Santiago Chile, January 9th to 13th 2017
Paper N° 3762
Registration Code: S-Y1463408380

ADVANCED NUMERICAL MODELS FOR SEISMIC DAMAGE ASSESSMENT OF RC COLUMNS

T. Tatar [1], M. Pimentel [2], J.M. Castro [3], M. Marques [4]

[1] *PhD Candidate, University of Porto, tuba.tatar@fe.up.pt*
[2] *Asst. Prof., University of Porto, mjsp@fe.up.pt*
[3] *Asst. Prof., University of Porto, jmcastro@fe.up.pt*
[4] *Post-Doctoral Researcher, University of Porto, mario.marques@fe.up.pt*

1. Abstract

The adequate modelling of the nonlinear cyclic demand of structural elements is deemed crucial to ensure a reduced level of uncertainty in the numerical estimates of the seismic behavior of structures. Usually, fiber-based or plastic-hinge models are considered when response history analyses are performed. Pros and cons emerge from the use of both models in what concerns to the identification of the local physical damage of the element, the global behavior of the structure and the corresponding computational time and complexity of the analyses. Moreover, the calibration of these models is not always straightforward, often leading to erroneous assumptions for the definition of the modelling parameters. Even when experimental data is used, questions arise in the calibration of these parameters with the intention to use an effective and systematic procedure for different structural elements.

The work presented in this paper addresses the definition of a comprehensive framework for the advanced numerical modelling of reinforced concrete members, using finite elements and nonlinear models for the concrete and steel materials. The accuracy of the modelling approach is assessed through comparisons with experimental results, considering several response parameters that represent the damage state of the element when it is subjected to monotonic and cyclic loading, such as, energy dissipation, chord rotation, crack width and extension, plastic hinge length, history of internal forces and deformations, etc.

Keywords: Seismic risk assessment; Damage, Engineering demand parameter

2. Introduction

This paper presents the first part of an ongoing project which directly associates costs of repair with physical damages in reinforced concrete frame buildings, in terms of engineering demand parameter(s) (EDP) under seismic load. The project consists of two phases: the first phase includes simulation of behavior of each structural component of a reinforced concrete (RC) frame building using detailed finite element analyses in order to correlate the physical damage with suitable engineering demand parameter(s) which will be discussed in the present paper. The second phase involves the assessment of the structural performance of RC frame buildings, using 2D models (hinged or distributed plasticity) in order to compute the economic loss of structures based on the EDP(s) values, which in the first phase of the work have demonstrated high correlation with the physical damages.

In current earthquake loss assessment approaches, damage is commonly defined base on ductility ratio or dissipated energy and usually related with either global or local indices [1-5]. The indices can provide vulnerability of the structure, performance evaluation of the structure and decision regarding to rehabilitation of the structure. Even though the indices are able to capture non damaged and severely damaged status, they, however, poorly provide accurate results for intermediate damage states, which is the most critical stage regarding of strengthening decision [6]. To improve the accuracy of economic loss predictions in RC frame buildings, the damage scales are redefined by experts according to the physical damages and cost of repair are defined according to the applied repair techniques [7].Therefore, four damage classes where included in this study slight, moderate, severe and collapse. Their physical and visible damages and repair techniques are shown in Table 1. The aim of the work is to be able to detect those defined visible damages via numerical modeling and to correlate the defined physical damage with engineering demand parameter which can also be represented within 2D analysis.

A reliable analytical model shall enable to describe the behavior of the structure and to simulate the physical damages that are experienced by each element, so that it is possible to compute accurately the repair costs of the structure. The paper will be focused on only capturing physical damages in reinforced concrete columns through finite element models, including crack width, spalling etc.

Table 1 – Damage classes, visible damages and their repair techniques [7]

Damage Class	***Visible Damage***	***Repair Techniques***
Slight	Hairline cracking (w<0.1mm)	Paint, plaster, rub epoxy resin
	Cracking (0.1mm<w<0.8mm)	Epoxy resin injection
Moderate	Crushing concrete in the joint + light spalling	Epoxy resin injection, Reposition of the detached volumes with structural mortar
	Spalling	RC jacketing, Reposition of the detached volumes with structural mortar or concrete, + Steel plates or stripes application or + CFRP localized jacketing
Severe	Buckling of bars	Replacement of the buckled/fractured bars + CFRP localized jacketing or + steel localized jacketing or strapping, Replacement of the damaged element
	Fracture of bars	
Collapse	Element completely out of its original position	No repairing, demolition and cleaning works.

3. Material Properties and Modeling

In this study, five columns were assessed and numerically modeled using the software, DIANA 9.6. These specimens were previously tested in laboratory: one (UP) was performed at University of Porto [8] and the remaining ones (V1, V2, V3 and V4) were, selected from literature which have the same material and geometrical properties, however, subjected to the different axial load levels [9]. The properties of the specimens are summarized in Table 2. To improve the accuracy when capturing all the aforementioned physical damages in a single finite element model, a brick element with 27 gauss points (CHX60) is used and the rotating smeared crack model is also employed for the concrete material. In order to include the degradation due to buckling of the

reinforcement bars, Dhakal-Maekawa constitutive model which explicitly commences post-yield buckling of bars is introduced to steel [10].

Table 2 – Physical and material properties of specimens

Specimen No.	***Section*** mm^2	***Height of the column*** mm	f_c' N/mm^2	f_y N/mm^2	***Axial Load*** kN	***Long. Rein.***	***Stirrups*** $Ø/mm$	***Rein. Ratio*** (ρ) %	***Mech. Rein.Ratio*** (ω) %
UP	200x400	1500	48	436	170	6Ø12	Ø6/150	0.85	0.08
V1	300x300	1100	30	344	0	12Ø13	Ø6/70	1.77	0.20
V2					310				
V3					620				
V4					930				

Figure 1 shows the FE models of the specimens, the red lines in (a) and (c) represent the reinforcing bars and (b) and (d) illustrate the meshed models. All the specimens are analyzed under monotonic loading.

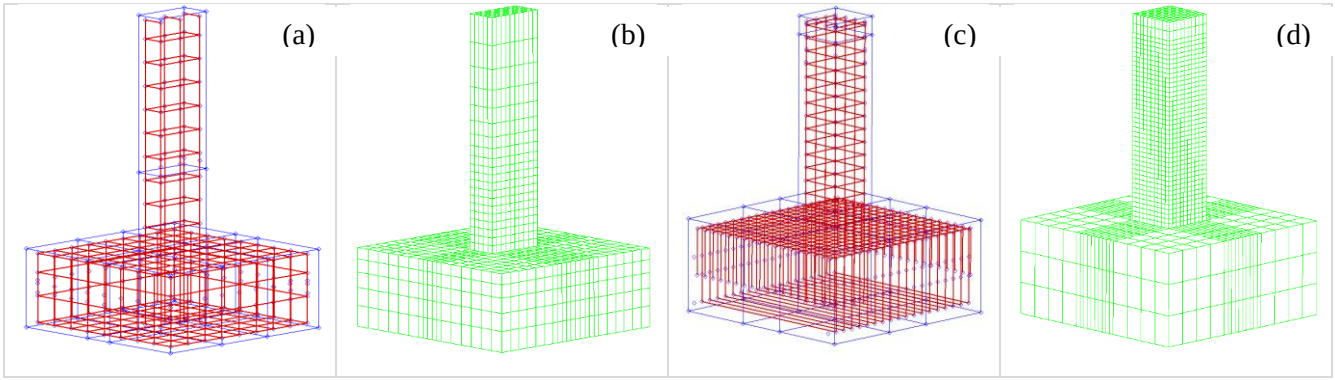

Figure 1– Reinforcement and mesh of the models (a and b represent UP, c and d illustrate V1, V2, V3 and V4)

4. Calibration Process

Calibrating the material properties and evaluating the crack pattern with the experiments in the numerical analyses are crucial for this study since the work is greatly relied on linking the physical damages with suitable engineering demand parameter(s) such as drift, total rotation etc. which shall be also representative on 2D simplified models. Hence, the calibration process has been done into two steps which are comparison of global response (global sense) in terms of shear vs. displacement and crack pattern (local sense). Thus, in global sense, the calibration of the material properties consists of four steps, which are: mesh sensitivity, compression fracture energy, bond-slip investigations and geometric nonlinearity.

4.1. Mesh sensitivity

Three different mesh sizes were considered and analyzed for the two sets of specimens, namely:

1. V1, V2, V3 and V4:

   25x25x30 mm^3, 50x50x60 mm^3 and 100x100x100 mm^3 respectively for fine, medium, coarse volumes;

2. UP:

   40x35x40 mm^3, 67x70x80 mm^3, 67x140x200 mm^3 respectively for fine, medium and coarse volumes.

The results from this sensitiveness study are shown in Figure 2. Even though the models with medium sized meshes are able to obtain response objectivity, i.e. results that are independent of the mesh size, due to stability reasons throughout the further investigations, the fine mesh size is selected for all the models. The effect of the axial load level on the objectivity of the response is observed and if the axial load however increases, the failure of the column occurs earlier due to prior concrete crashing resulting with a decrease in ductility.

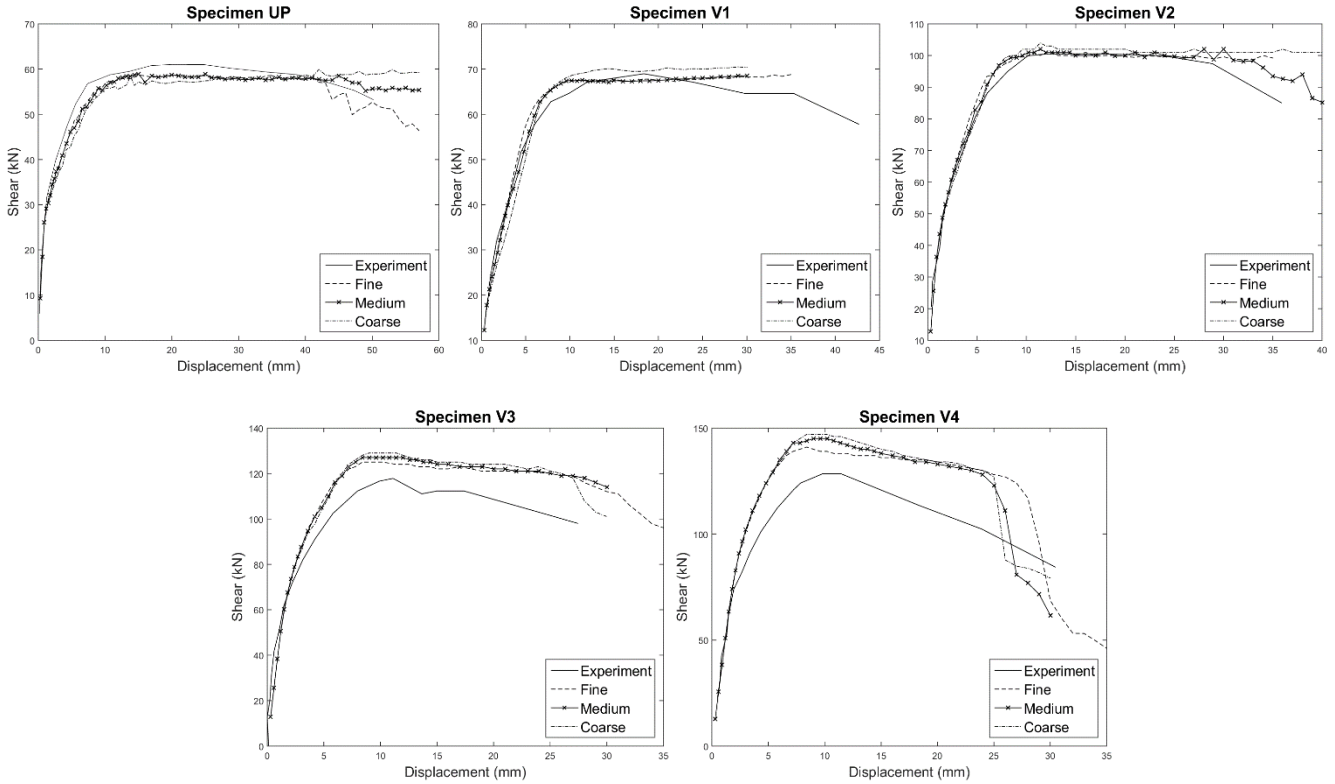

Figure 2– Mesh sensitivity investigation

4.2. Compression fracture energy (G_c)

In order to capture the post-peak behavior of the columns, the models with various compression fracture energy values are analyzed. The first estimated compression fracture energy value is calculated using the area of uniaxial stress-stain diagram after the peak multiplying by the crack bandwidth and then it is gradually increased until the ductility of the specimen is captured. Figure 3 presents the responses of the columns in terms of shear vs. displacement. The influence of the compression fracture energy can be observed after the peak point and the ductility improves by increasing the G_c value. Because the value of 80 N/mm for V1, V2, V3 & V4 and 50 N/mm for UP are able to simulate the ductility of the experimental tests, the following investigations have been proceeded using these values. The effect of this parameter can be noticeably seen when the specimen is subjected to higher axial load level, such as in case of column V4. In addition, since the concrete failure is not detected in V1, the different values of G_c produce similar results.

4.1. Bond-slip effect in global response & geometric nonlinearity

The bond-slip effect is calculated according to the FIB proposal as a function of confinement effect and bond condition, and four possible scenarios are investigated in this work which are confined-good bond, confined-other bond, unconfined-good bond and unconfined-other bond conditions [11]. Figure 4 demonstrates the impact of bond-slip with four aforementioned conditions and, in addition, the response from experimental tests and the results of the models without bond-slip effect are also included. The selection of the bond and the confinement condition has been done in terms of global response and crack pattern, and the most suitable condition which is

confined and other bond for the examples is selected. The influence of bond-slip would be explicitly noticed before and after yielding of reinforcing bars. Moreover, increase in ductility is observed after including bond-slip phenomena into the models while a small reduction in strength around the yielding point of the bars can be perceived. In addition to all, the second order effect due to horizontal load is considered at this step and obtained more consonant results to the experiments.

4.2. Numerical Failure of the Specimens

The failure of the experimental and numerical results (including geometric nonlinearity, bond-slip effect and the Dhakal-Maekawa buckling model) are compared and shown in Figure 5. Beside of V1 in which there is neither concrete crushing nor reinforcement bar buckling, the specimens show very good agreement in the numerical analyses comparison to the experimental failure.

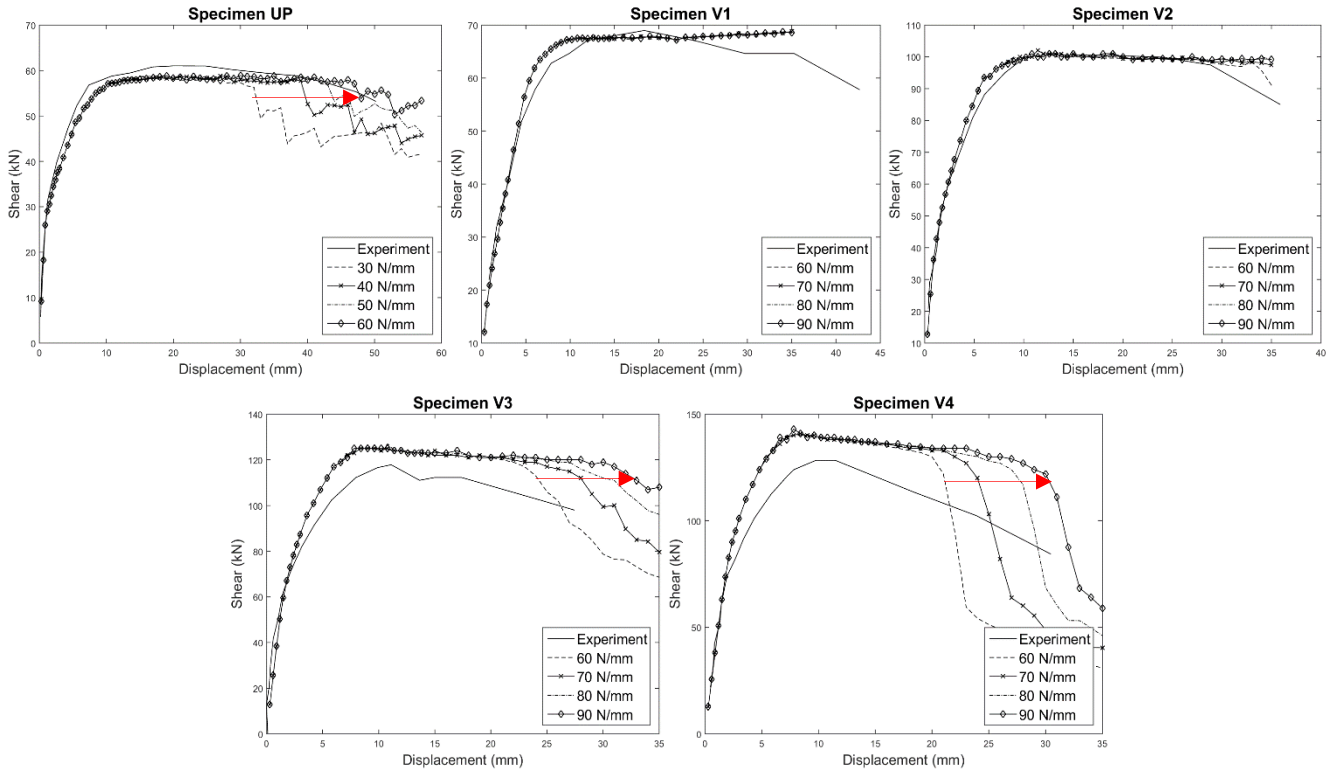

Figure 3 – Compression fracture energy investigation

5. Comparison of Crack Pattern and Damage Length

The following figures show the comparison of crack pattern of the models without and with bond-slip activation, along with the results from the experimental tests. Figure 6-10 show the crack patterns of the models without bond-slip activation and with slip activation and experimental results for V1, V2, V3, V4 and UP respectively. It can be clearly observed that all the models are able to produce the crack pattern fairly. Since the bond-slip model allows concrete and steel behave discretely, wider crack width especially at the bottom of the column and more localized cracks can be observed on the models with bond-slip effects which creates more realistic crack pattern all over the height of the columns. By the bond-slip model, the length of the damage zone is reduced while the cracks on the model without bond-slip are separated throughout the height. On the contrary, the crack length becomes more visible on the model with bond-slip. Moreover, increasing the axial load origins a reduction of the damage zone and length with the narrower crack widths.

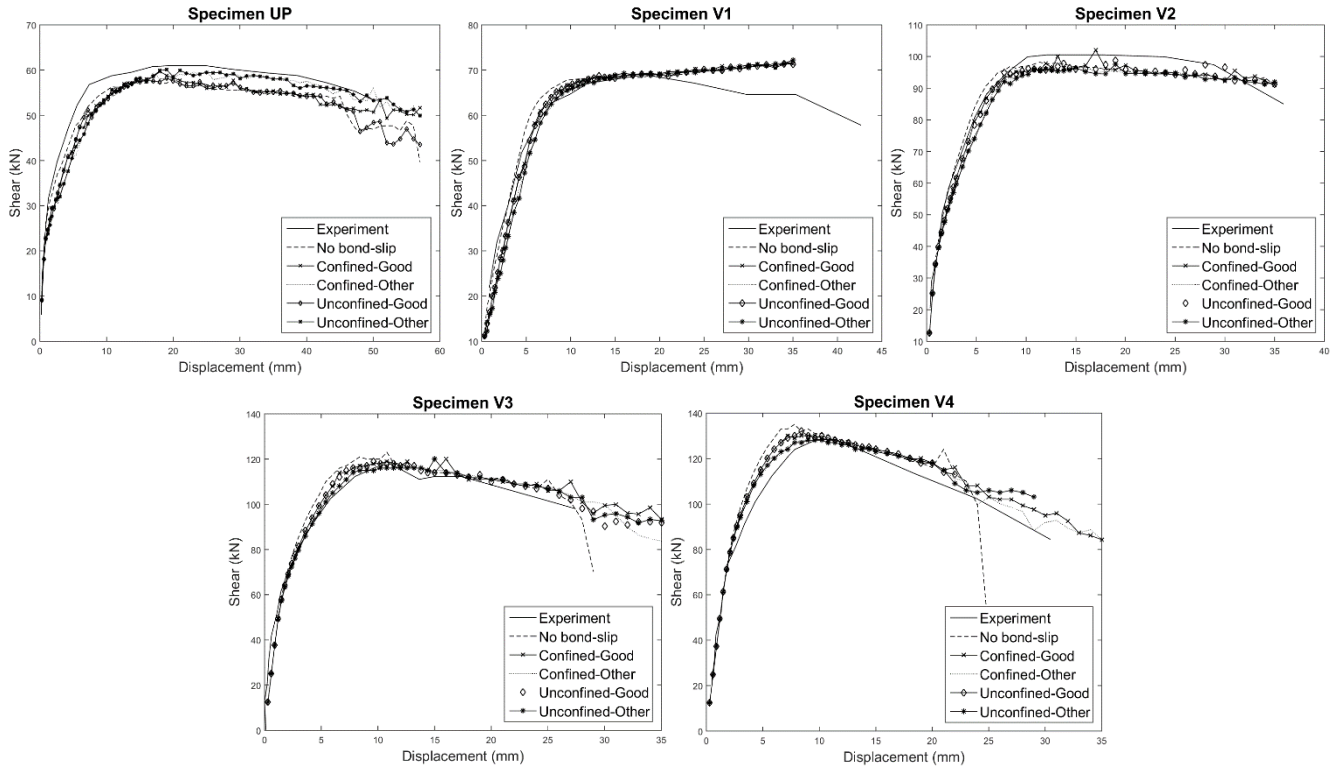

Figure 4 – Effect of bond-slip action

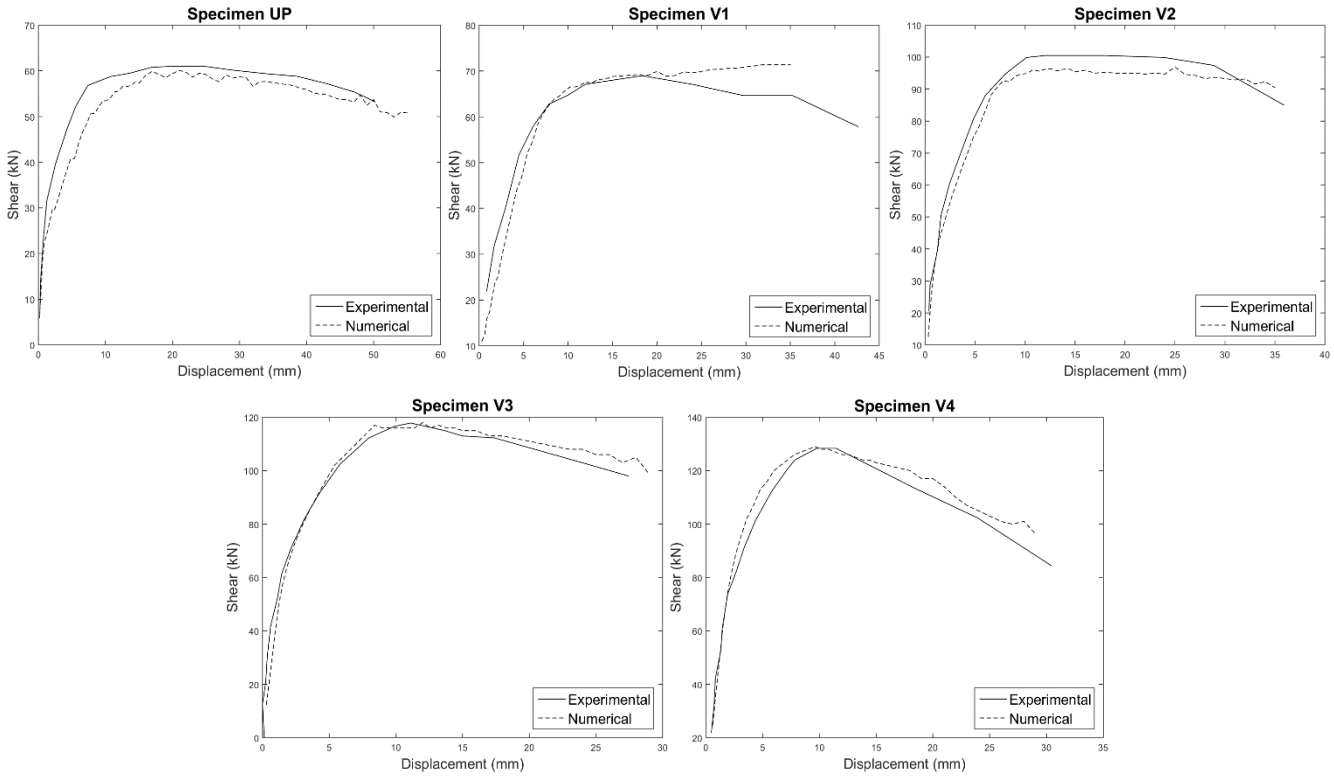

Figure 5– Experimental vs numerical failure of the specimens

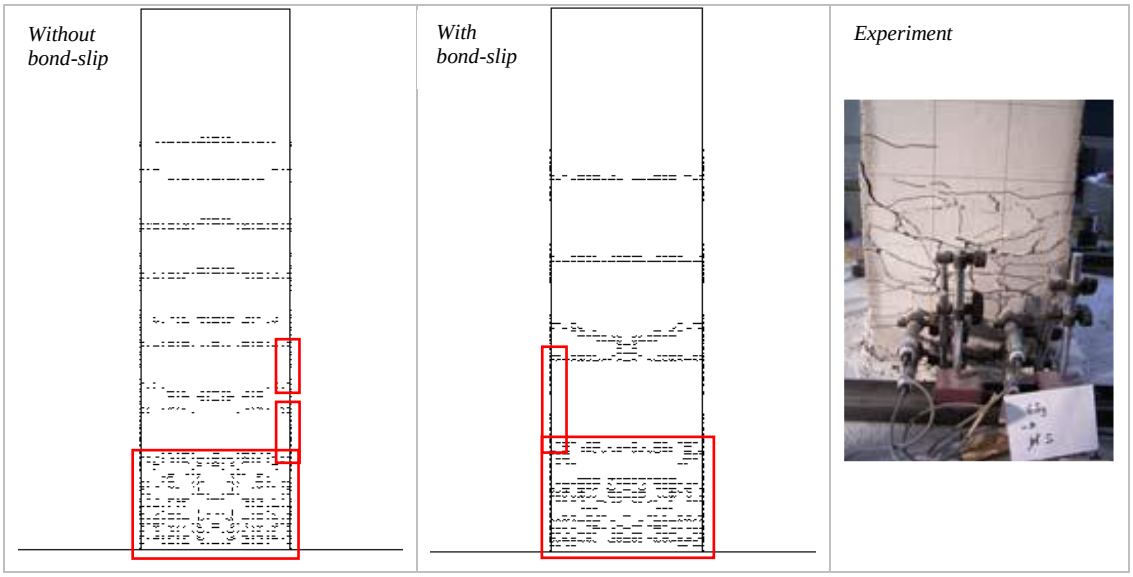

Figure 6 – Comparison of crack patterns of V1

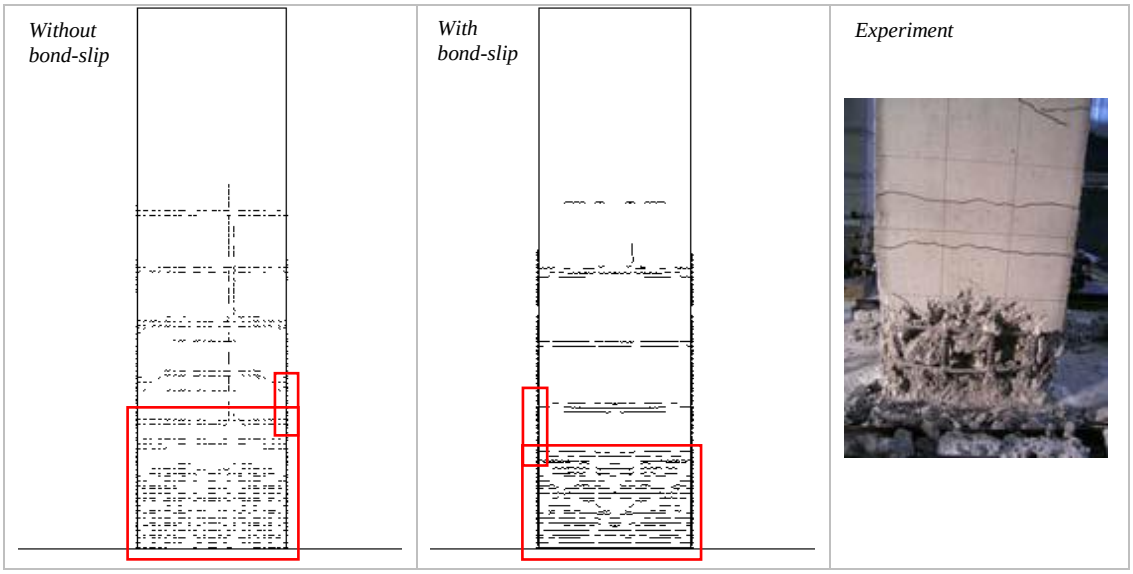

Figure 7 – Comparison of crack patterns of V2

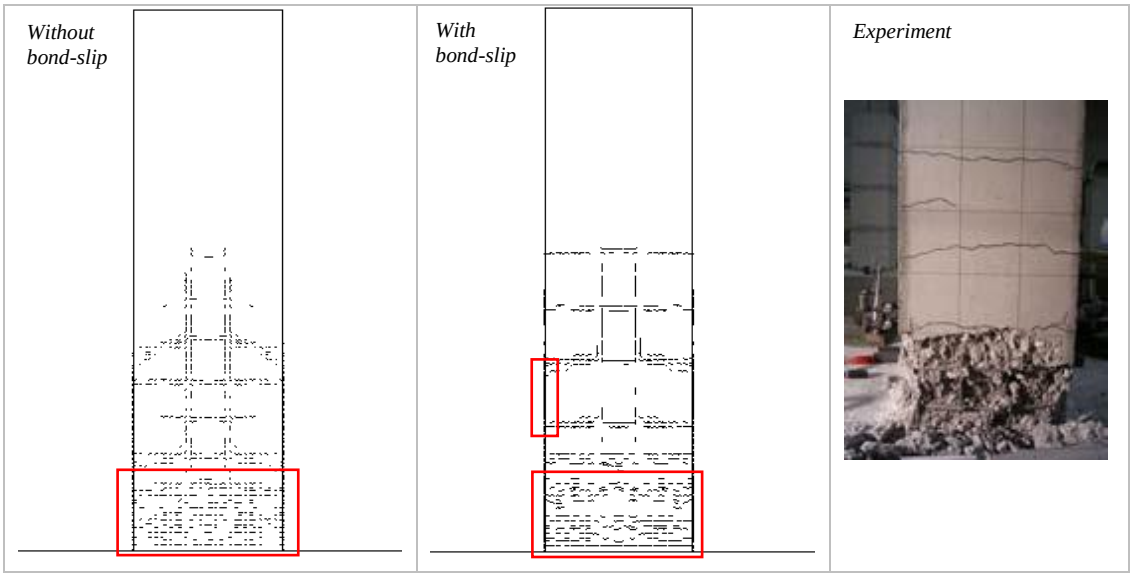

Figure 8 – Comparison of crack patterns of V3

Figure 9 – Comparison of crack patterns of V4

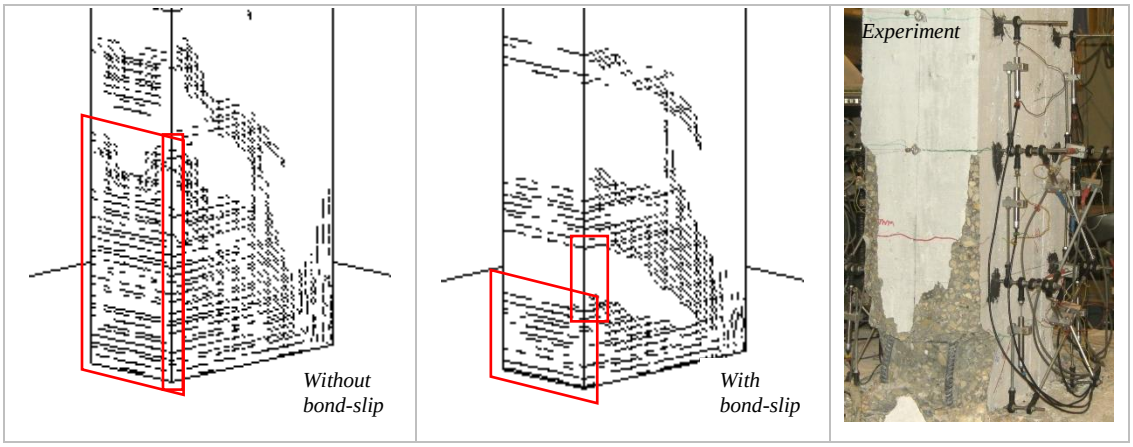

Figure 10 – Comparison of crack patterns of UP

6. Physical Damages vs Engineering Demand Parameters

While the physical damages are correlated with the engineering demand parameter(s), changes in response in local sense, such as; decreasing in axial load in a bar, a sudden drop in stress in concrete element, or the maximum stress in concrete element are associated with failure for concrete or steel material. The physical damages those observed in experimental results and captured in the numerical models described before are correlated with drift and total rotation. Although recognizing the limitations of considering these two indicators of the structural performance, it is noticeable that it will cover the vast majority of the seismic fragility studies and applications and therefore it can lead to an important contribution for the development of more accurate models and for the reduction of the associated uncertainty. For now, the paper will cover only two different crack widths and spalling of concrete as physical damages in detail.

6.1. Crack width investigation

The crack width is calculated pursuing relative displacement of the nodes along the corner elements and the evolution of the first three cracks (two for Up) for each specimen are shown in Figure 11. Once a crack width reaches the 0.1 mm, which is a value that a crack starts to be visible, the corresponding load step is considered as a starting point of a new limit state and calculated in terms of drift and total rotation of the column. The same procedure is followed for the crack width of 0.8 mm. In addition, an influence of axial load is detected on crack development and by increasing compression on a column, a delay on onset of cracks is occurred, for instance; the cracks form in V1 immediately after facing the horizontal load. However, the cracks in V4 which has the highest axial load level in this work form later than the other specimens.

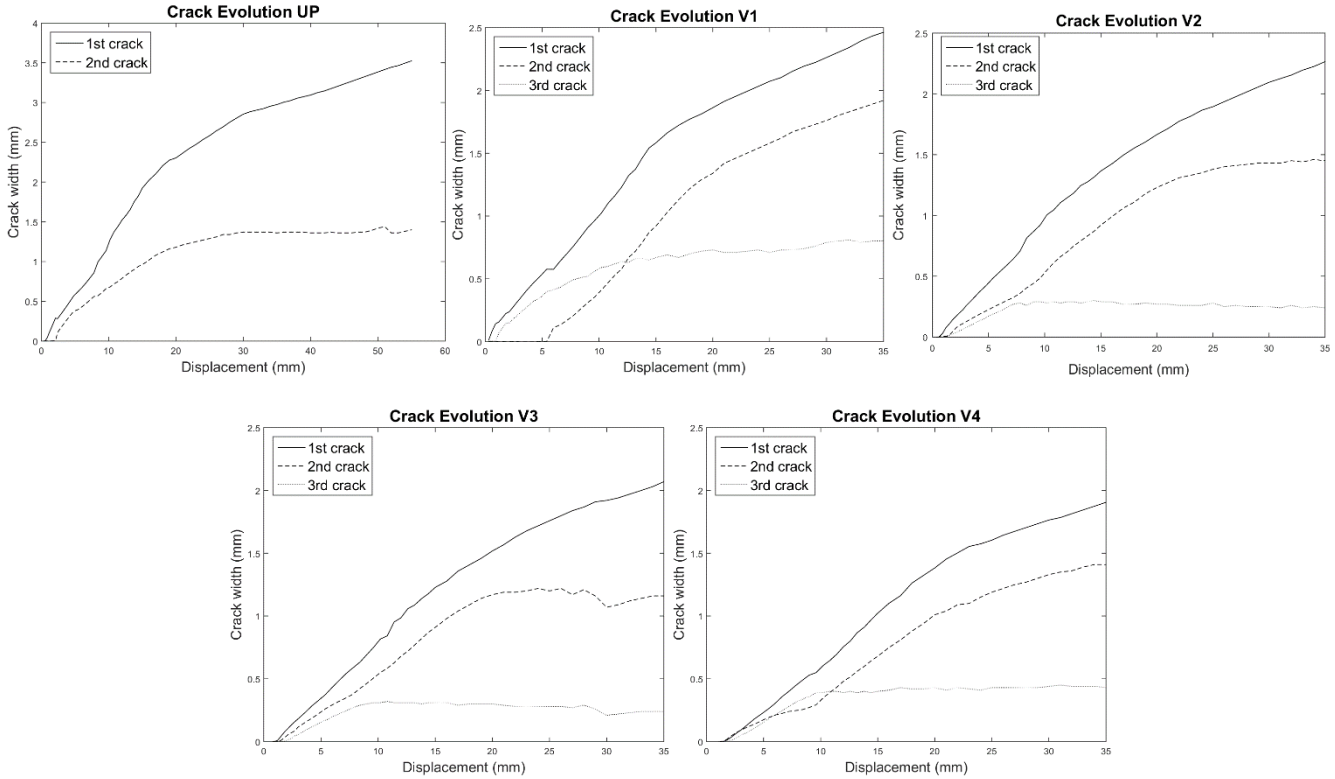

Figure 11 – Crack evolution in the models

6.2. Spalling of concrete

The investigation of spalling is based on tracking the load step until the concrete element crushes which is assumed as a sudden drop in stress. The first ten corner elements along the height (approximately equal to the plastic hinge

length) are investigated in terms of stress and displacement. Figure 12 illustrates stress evolution of the first ten elements for each specimen. Each line represents one element and red lines show failed elements and green lines demonstrates stable elements. Table 3 summarizes the extent of the damage obtained from numerical analyses and experimental tests. It is clearly seen that the numerical models are able to simulate the damage length and represent the phenomenon of concrete spalling which also validates the abovementioned assumption (drop in stress).

Table 3 – Comparison of damage length

	Experimental *(cm)*	***Numerical*** *(cm)*	***Difference*** *(cm)*
UP	15	17.5	+2.5
V1	N/A	-	-
V2	≈20	20	-
V3	≈20	20	-
V4	14.5	17.5	+3.0

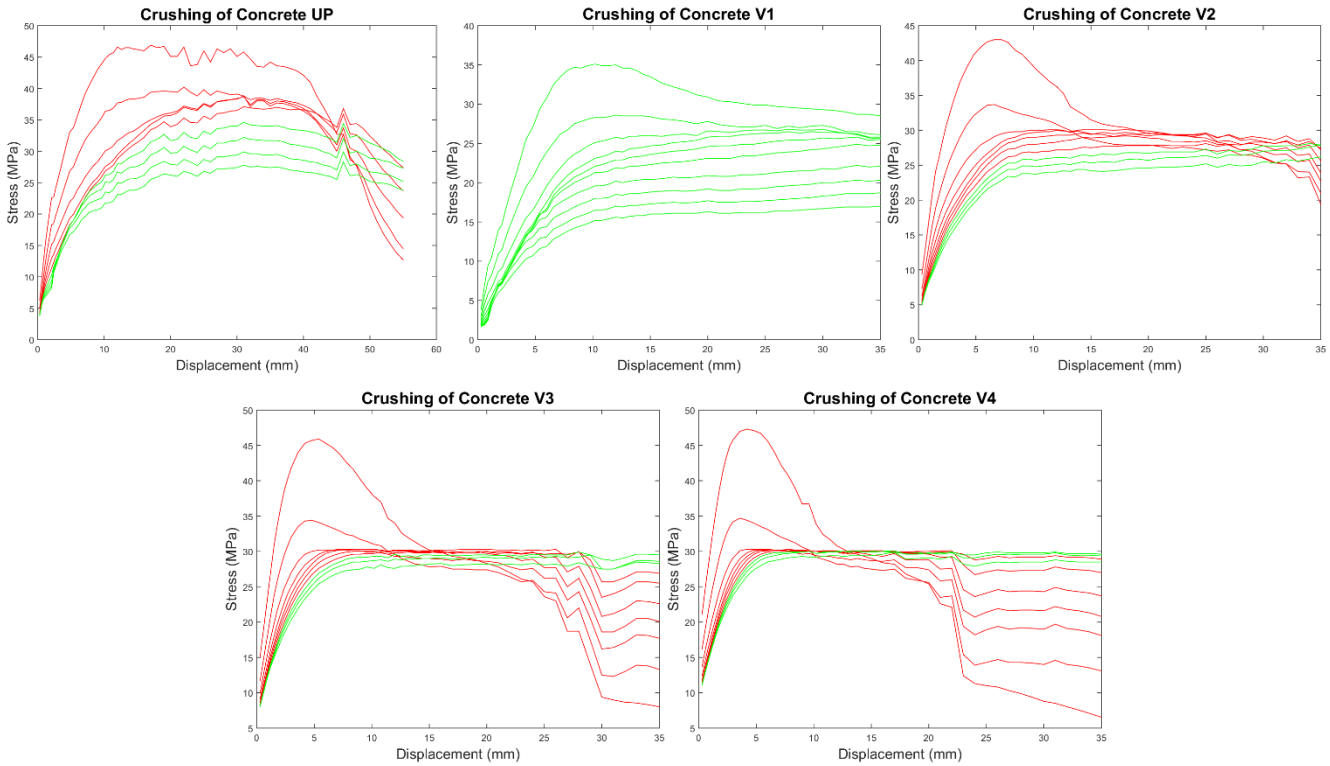

Figure 12 – Crushing of the corner elements

6.3. Correlation of physical damage with engineering demand parameter(s)

The assessment of suitable EDPs is the last and crucial step of the present work, in order to guarantee that the physical damages and corresponding limit states are duly characterized. As previously referred, these parameters will be applied in the future developments of this study on the seismic structural performance assessment of reinforced concrete elements using simplified frame models. Therefore, drift and total rotation are selected as EDPs. Figure 13 demonstrates the evolution of the visible damages in terms of capacity curves (total base shear vs displacement) of the two sets of specimens. Visible cracks (w<0.1mm) occur before the maximum response

and depends on the axial load level, wide cracks (0.1mm<w<0.8mm) can form before and after maximum response. Spalling of concrete are postponed by decreasing the axial load level. Table 4 and

Table **5** give a summary of all the damage states in terms of drift and total rotation, respectively, which correspond to the preliminary proposal for the limit states of damage that can be observed in a RC column.

Table 4 – Damage states in terms of drift

	w<0.1	***w<0.8***	***Spalling***
UP	0.08%	0.52%	2.67%
V1	0.08%	0.76%	-
V2	0.14%	0.76%	2.91%
V3	0.19%	0.98%	2.18%
V4	0.33%	1.15%	1.82%

Table 5 – Damage states in terms of total rotation

	w<0.1	***w<0.8***	***Spalling***
UP	0.0006	0.0044	0.0255
V1	0.0007	0.0063	-
V2	0.0010	0.0057	0.0272
V3	0.0013	0.0076	0.0200
V4	0.0024	0.0101	0.0169

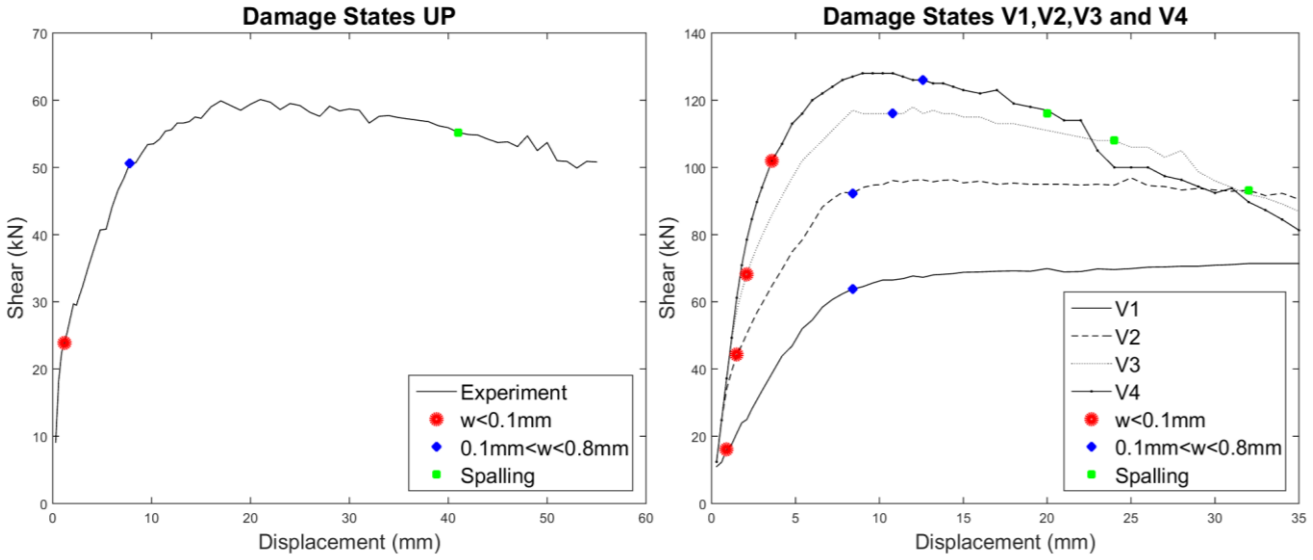

Figure 13 – Physical damages in global response

7. Conclusions and Future Work

Five experimental tests are numerically modeled and analyzed in this work in order to correlate physical damages with engineering demand parameter(s) via finite element approach. Through calibration process, mesh sensitivity,

compression fracture energy, geometric nonlinearity and bond-slip effects are explored and their influences onto the models are discussed. The flowing conclusions are obtained in terms of calibration process:

1. In this work, even though objectivity is achieved using medium size mesh, fine size mesh is used due to stability consideration and further buckling investigation,
2. Influence of compression fracture energy can be observe if there is concrete failure and it improves the ductility of the column,
3. The impact of bond-slip can be observed before and after yielding of bars in global response even though small reduction in strength would be noticed and it critically changes the crack pattern,
4. An improvement in ductility is detected in the models after activating bond-slip action.

In order to establish a correlation between visible damage and engineering demand parameter(s), concrete and steel elements are investigated in local sense in terms of stress, displacement etc. Crack widths are calculated using relative nodal displacement and spalling existence is assumed when the concrete elements crushed. The physical damages from numerical analyses and experiments impartially match and are related with two engineering demand parameters which are drift and total rotation.

Light spalling and buckling have been investigating and will be correlated with the current and additional EDPs at the ultimate point of the first phase of the work.

8. References

[1] A. Cakmak and E. DiPasquale, "Detection and Assessment of Seismic Structural Damage," 1987.

[2] Y. Chung, C. Meyer, and M. Shinozuka, "Seismic damage assessment of reinforced concrete buildings," in *Report No. NCEER-87-0022*, ed: National Center for Earthquake Engineering Research, State University New York at Buffalo, 1987.

[3] Y.-J. Park and A. H.-S. Ang, "Mechanistic seismic damage model for reinforced concrete," *Journal of structural engineering*, vol. 111, pp. 722-739, 1985.

[4] M. S. Williams and R. G. Sexsmith, "Seismic damage indices for concrete structures: a state-of-the-art review," *Earthquake spectra*, vol. 11, pp. 319-349, 1995.

[5] Y. Nakano, M. Maeda, H. Kuramoto, and M. Murakami, "Guideline for post-earthquake damage evaluation and rehabilitation of RC buildings in Japan," in *13th World Conference on Earthquake Engineering*, 2004.

[6] R. Sinha and S. Shiradhonkar, "Seismic Damage Index for Classification of Structural Damage–Closing the Loop," in *Proceedings of the Fifteenth World Conference on Earthquake Engineering*, 2012.

[7] "Earthquake Loss Assessment of the Portuguese Building Stock," University of Porto2014.

[8] H. Rodrigues, "Biaxial Seismic Behavior of Reinforced Concrete Columns," Doctoral Dissertation, Civil Engineering, University of Aveiro, Aveiro, 2012.

[9] T. Denpongpan and H. Shima, "Effect of Axial Load on Ductility of Reinforced Concrete Columns," presented at the OUR WORLD IN CONCRETE & STRUCTURES, Singapore, 2005.

[10] R. P. Dhakal and K. Maekawa, "Modeling for postyield buckling of reinforcement," *Journal of Structural Engineering*, vol. 128, pp. 1139-1147, 2002.

[11] F. I. du Béton, "Bond of reinforcement in concrete: state-of-art report," *Lausanne, Switzerland: International Federation for Structural Concrete*, p. 427, 2000.